Entanglement and Quantum phase transition in topological insulators

Prasanta K Panigrahi,* Anvesh Raja K, and Anant Vijay
Indian Institute of Science Education and Research Kolkata, Mohanpur, 741246, West Bengal, India

Bhavesh Chauhan
Physical Research Laboratory, Navrangpura, Ahmedabad, 380009, Gujarat, India.
(Dated: April 4, 2017)

Presence of entangled states is explicitly shown in Topological insulator (TI) Bi_2Te_3. The surface and bulk state are found to have the different structures of entanglement. The surface states live as maximally entangled states in the four-dimensional subspace of total Hilbert space (spin, orbital, space). However, bulk states are entangled in the whole Hilbert space. Bulk states are found to be entangled maximally by controlled injection of electrons with momentum only along the z-direction. Scheme to detect entanglement in a 2-D model using measurement, confirming natural implementation of universal Hadamard with Controlled-NOT gates is explicated.

arXiv:1704.00579v1 [quant-ph] 3 Apr 2017

I. INTRODUCTION

Creating and entangling single qubits, their scalability and protection against decoherence are key to the realization of quantum devices and quantum computers. In this regard, superconducting qubits [1], quantum dots [2] and nitrogen defect in diamond have shown promise [3]. In the absence of perfect isolation from surroundings, the above systems are prone to decoherence, which limits their applicability [4]. In recent times, topological quantum computation with the underlying states protected by topology has attracted attention because of its robustness against decoherence [5]. Interestingly, topological insulators exhibit topologically protected surface states [5–9], and have found applications in spintronics [10] and electrical memory devices [11–13]. Here, we demonstrate realization of entangled qubits and controlled variation of entanglement with parameter tuning. For specificity we have considered Bi_2Te_3, however, our approach is applicable to other 3-D gapped topological insulators.

Topological insulators are characterized by wavefunctions with coupled spin, orbital, and spatial degrees of freedom. Entanglement between orbital and spin degree of freedom naturally arises in such systems due to spin-orbit coupling. Consequently, level crossing occurs between corresponding pairs of states. A quantum phase transition (QPT) separates the topologically non-trivial phase, from its trivial counterpart. The nature of coupling of the three degrees of freedom is expected to be different for the conducting surface and the insulating bulk state, and also in trivial and non-trivial phases. In case of Bi_2Te_3, one can project the system into a subspace spanned by the the four states $\left|P1^+_-,+\frac{1}{2}\right\rangle, \left|P2^-_+,+\frac{1}{2}\right\rangle, \left|P1^+_-,-\frac{1}{2}\right\rangle, \left|P2^-_+,-\frac{1}{2}\right\rangle$ with the kinetic term (spatial part) arising perturbatively through the $\vec{k}\cdot\vec{p}$ perturbation expansion [14]. This results in Dirac type Hamiltonian with a Clifford algebra structure. Keeping in mind the entangled structure of the Hilbert space for TI and its role in QPT, we carry out a systematic investigation of the parameters affecting the entanglement and its behavior in trivial and non-trivial phases. It is also required for their possible use in quantum computation and other device applications. Here, we explicate the formation of entangled states in the 3D TI Bi_2Te_3 model.

The paper is organized as follows: In Sec-II we present the model for Bi_2Te_3 and obtain energy spectra for surface and bulk states. Sec-III deals with QPT at Γ point and entanglement characteristics as a function of Hamiltonian parameters. Sec-IV explicates a scheme to study entanglement using conductance measurement in a 2-D system of the underlying state. The last section is devoted to concluding remarks and future directions of work.

.

II. MODEL HAMILTONIAN

The minimum model Hamiltonian for Bi_2Te_3 with four states $\left|P1^+_-,+\frac{1}{2}\right\rangle, \left|P2^-_+,+\frac{1}{2}\right\rangle, \left|P1^+_-,-\frac{1}{2}\right\rangle, \left|P2^-_+,-\frac{1}{2}\right\rangle$ as basis, can be written as [15–17]:

$$H(\mathbf{k}) = \epsilon(\mathbf{k}) + \begin{bmatrix} M(\mathbf{k}) & A_2k_+ & 0 & A_1k_z \\ A_2k_- & -M(\mathbf{k}) & A_1k_z & 0 \\ 0 & A_1k_z & M(\mathbf{k}) & -A_2k_- \\ A_1k_z & 0 & -A_2k_+ & -M(\mathbf{k}) \end{bmatrix} \quad (1)$$

where $k_\pm = k_+ \pm ik_y$ and,

$$\epsilon(\mathbf{k}) = C + D_1(k_z^2) + D_2(k_z^2 + k_y^2) \quad (2)$$

$$M(\mathbf{k}) = M - B_1(k_z^2) - B_2(k_z^2 + k_y^2) \quad (3)$$

$$(4)$$

It differs from the Dirac Hamiltonian as it contains the parabolic band term Bk^2, changing the Z_2 topological index from zero to one [18]. Here, $P1^+_-$ and $P2^-_+$ are two hybrid orbitals near the Fermi surface. Due to larger

* panigrahi.iiser@gmail.com

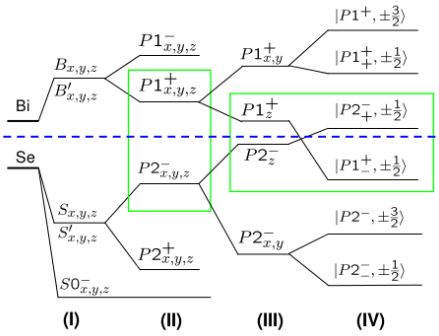

FIG. 1: Schematic diagram of the band structure of Bi_2Se_3, depicting four steps of energy levels splitting: (I) the hybridization (II) bonding and anti-bonding (inversion symmetry), (III) crystal field splitting and (IV) the SOC.

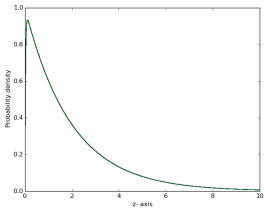

FIG. 2: *Probability distribution of the surface state along z-axis for parameters values* $A_2 = 4, M = 2 \& B = 0.1$.

principal quantum number of Bi compared to Te, its energy levels lies in conduction band. The total angular momentum along the z-direction is conserved after taking into account spin-orbit coupling (SOC). Hybridization only occurs between the states $|\Lambda, p_z, \uparrow\rangle$ & $|\Lambda, p_+, \downarrow\rangle$ and $|\Lambda, p_z, \downarrow\rangle$ & $|\Lambda, p_-, \uparrow\rangle$ (where $\Lambda = P1^+_-, P2^-_+$), which leads to level crossing between pair of states $\left|P1^+_-, \pm\frac{1}{2}\right\rangle$ and $|P2^-_+, \pm\frac{1}{2}\rangle$ (see FIG.1).

For the bulk eigenstates, we start with the ansatz $\Psi(k) = e^{-i(\omega t - k_x.x - k_y.y)}\phi_j(k_z)$, which comprises of plane waves along x- and y- direction and four component spinorial part $\phi_j(k_z)$. Using the fact that the electrons can be injected in the media in a particular momentum state such that the system is in the k_z eigenstate ($k_x = k_y = 0$), energy dispersion for (1) is given by $E = \pm\left[(M - Bk_z^2)^2 + (Ak_z)^2\right]^{1/2}$. Two orthogonal doubly degenerate eigenstates $\phi_j(k_z)$ for this system corresponding to eigenvalues $\pm E$ are given as:

$$\left(\frac{M(\mathbf{k_z})\pm E}{Ak_z} \;\; 0 \;\; 0 \;\; 1\right)^T; \left(0 \;\; \frac{M(\mathbf{k_z})\pm E}{Ak_z} \;\; 1 \;\; 0\right)^T.$$

These states are not separable in any of the three different subspaces. The surface states (zero energy) solutions can be obtained by applying boundary condition in real space coordinates normalized to half surface $0 \leq z \leq \infty$:
$\Psi(x, y, z, t) = N_s\phi_{1,2}(z)e^{-i(p_x x - p_y y)}$,
where $\phi_1(z) = (e^{-\lambda_- z} - e^{-\lambda_+ z})\left(0 \;\; \pm i \;\; 1 \;\; 0\right)^T$;
$\phi_2(z) = (e^{-\lambda_- z} - e^{-\lambda_+ z})\left(1 \;\; 0 \;\; 0 \;\; \pm i\right)^T$ and
$N_s = \frac{\sqrt{\lambda_+\lambda_-(\lambda_+ + \lambda_-)}}{(\lambda_+ - \lambda_-)}$; $\lambda_\pm = \frac{A}{2B} \pm \frac{\sqrt{A^2 - 4MB}}{2B}$. Curvature parameter B controls the location of this zero energy state from the boundary. Increasing B from 0.1 to 1 shifts $|\Psi|_{max}$ from 0.1 to 0.6 along +z-axis and $|\Psi|_{max}$ value decreases to half, as depicted in FIG.2.

III. QUANTUM PHASE TRANSITION (QPT) AND ENTANGLEMENT

We now analyse entanglement properties of finite energy bulk states, as the zero energy states are maximally entangled in the four dimensional subspace, being separable in spatial degree of freedom. As is well known entanglement has close connection with quantum phase transition (QPT) [19, 20], which occurs when the ground state of a system changes by varying parameters such as magnetic field, pressure, etc [21, 22]. This leads to change in the symmetry of the ground state. For the above mentioned model symmetry changes by band closing and reopening as sign of M/B is changed (see FIG.3. below).

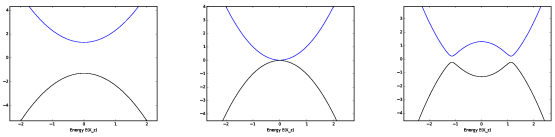

FIG. 3: *Plot showing the band structure along z-direction. Gapped band structure before QPT i.e.,* $M/B < 0$ *(left), at QPT* $M/B = 0$ *(center) and band inversion for case* $M/B > 0$ *; with* $M = \pm 1.3 \& 0; B = 1; A = .2$.

A. Concurrence and quantum phase transition

Among the several measures to extract the signature of QPT [9, 23, 24] in solid state systems mentioned in [25, 26], we employ concurrence [27] as tool [28]. It gives the amount of state overlap and for the present system is given by (for both $E, -E$):

$$\mathcal{C}_\pm = \frac{1}{2}max\{0, \frac{1}{\sqrt{N_\pm}}(\frac{M(\mathbf{k}) \pm E}{Ak})\} \qquad (5)$$

The orthogonal states mentioned in last section are pure states and can be designated as follows:

$$\phi_{\pm 1}(k) = \frac{1}{\sqrt{N_\pm}}(a_\pm |00\rangle + |11\rangle) = \frac{1}{\sqrt{N_\pm}} \begin{pmatrix} a_\pm \\ 0 \\ 0 \\ 1 \end{pmatrix} \quad (6)$$

$$\phi_{\pm 2}(k) = \frac{1}{\sqrt{N_\pm}}(a_\pm |10\rangle + |01\rangle) = \frac{1}{\sqrt{N_\pm}} \begin{pmatrix} 0 \\ a_\pm \\ 1 \\ 0 \end{pmatrix} \quad (7)$$

With $N_\pm = 1 + a_\pm^2$ and $a_\pm = \frac{M(\mathbf{k}) \pm E}{Ak}$ being normalization constants. One can see in the concurrence plot (FIG.4. upper panel) that for small values of B, it increases and attains the maximum value of one at the critical point B_c. B_c corresponds to phase transition point. For higher values all states become separable, thus changing the ground state of the system and revealing the presence of QPT. Changing the sign of M (black curve) is equivalent to phase transition.

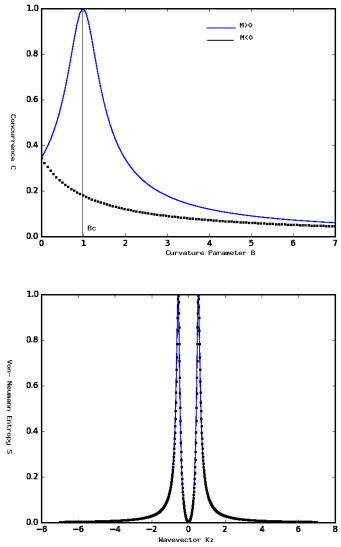

FIG. 4: *Concurrence plot as a function of B (upper panel). Dark line corresponds to $M > 0$ and dashed line corresponds to $M < 0$ respectively(above plot). Entropy variation with wave vector k_z showing maxima at $\pm\sqrt{(\frac{M}{B})}$ (below plot).*

In summary, M and B are the parameters that controls phase transition and concurrence ($\mathcal{C}$) is maximum if $M/B > 0$. Parameter M represents the mass term, which can be tuned by external electric field or doping, whereas B is the curvature parameter. This Hamiltonian describes a trivial insulator for $\frac{M}{B} < 0$. However, when $\frac{M}{B} > 0$ the bands are inverted leading to a TI. It may be noted that von Neumann entropy $\rho = (\frac{1}{\sqrt{N}})^2 \log_2(\frac{1}{\sqrt{N}})^2$ provides the same results and we get entropy maxima at momenta $k = \pm\sqrt{\frac{M}{B}}$. The corresponding states at these values become $\phi_1(z) = \sqrt{\frac{1}{2}} \begin{pmatrix} 0 & \pm 1 & 1 & 0 \end{pmatrix}^T$ (Bell states).
.

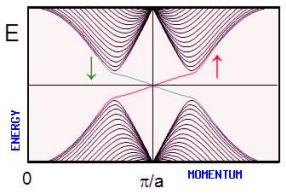

FIG. 5: *Schematic of band dispersion in 2-D lattice. Two crossing (red & green) branches correspond to a pair of edge states with opposite spin helicities $= \pm 1$.*

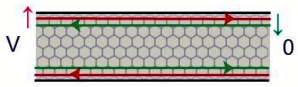

FIG. 6: *Schematic diagram of 2-D TI ribbon showing the spin-up and spin-down states in terms of entangled states.*

IV. GATE IMPLEMENTATION

Utilization of the topological states for practical purposes requires measurement, which confirms the existence and amount of entanglement. We consider a 2-D TI model to describe a measurement scheme (see FIG.6.). The effective Hamiltonian for the model can be written as $\begin{bmatrix} h_+ & 0 \\ 0 & h_- \end{bmatrix}$, with $h_\pm = vp_x\sigma_x \pm vp_y\sigma_y + (mv^2 - Bk^2)\sigma_z$. At small values of k_x, zero energy solutions take the form $\Psi(x,y,z,t)_\pm = N_s\phi(y)e^{-ik_x x}$ & $\phi(y) = (e^{-\lambda_- y} - e^{-\lambda_+ y})$ $\begin{pmatrix} 0 & \pm i & 1 & 0 \end{pmatrix}^T$. Here, σ_i's do not represent real spin. However, $\Psi(x,y,z,t)_\pm$ are almost polarized along one direction of electron spin. Hence, Pauli matrices can be regarded approximately as real spin matrices. These edge states then can be distinguished as orthogonal eigenstates of helicity operator $\Sigma = \tau_y \otimes \sigma_x$ [29].

$$\Sigma\Psi(x,y,z,t) = \tau\Psi(x,y,z,t) \qquad \tau = \pm 1.$$

In a small-scale semiconductor with a few modes, quasi-Fermi levels for $-k_x$ states and $+k_x$ states are notably different [30]. Net current flows along $+x$ direction due to difference between quasi-fermi levels of $|+k_x, \uparrow\rangle$ and $|-k_x, \downarrow\rangle$ edge states, when potential V is applied across the left side (FIG.6). For measurement one can choose a spin filter (which is equivalent to choosing a basis) at the right end followed by a current measurement. Allowing down spin state through the spin filter would then result in zero current. On the contrary, choosing up spin state would result $\frac{e^2}{h}$ value [31] as current measurement. A large number of repetitive measurements can confirm the existence of maximally entangled states.

V. CONCLUSION

In conclusion, the model Hamiltonian describing a 3-D topological insulator Bi_2Te_3 can host entangled states.

Surface states are maximally entangled in a sub-space, while bulk states are entangled in the whole space. However, we conclude that it is possible to realize Bell states in the bulk by controlled injection of electrons, at phase transition point. Measurement scheme shown using a 2-D model implies, natural implementation of quantum gates. Further investigations are required for non-destructive measurements of such states.

[1] John Clarke and Frank K Wilhelm. Superconducting quantum bits. *Nature*, 453(7198):1031–1042, 2008.

[2] Christoph Kloeffel and Daniel Loss. Prospects for spin-based quantum computing in quantum dots. *Annu. Rev. Condens. Matter Phys.*, 4(1):51–81, 2013.

[3] Thaddeus D Ladd, Fedor Jelezko, Raymond Laflamme, Yasunobu Nakamura, Christopher Monroe, and Jeremy L OBrien. Quantum computers. *Nature*, 464(7285):45–53, 2010.

[4] Ananda Roy and David P DiVincenzo. Topological quantum computing. *arXiv preprint arXiv:1701.05052*, 2017.

[5] Xiao-Liang Qi and Shou-Cheng Zhang. The quantum spin Hall effect and topological insulators. *Physics Today*, 63(1):33–38, 2010.

[6] B Andrei Bernevig and Shou-Cheng Zhang. Quantum spin Hall effect. *Physical Review Letters*, 96(10):106802, 2006.

[7] Charles L Kane and Eugene J Mele. Quantum spin Hall effect in graphene. *Physical Review Letters*, 95(22): 226801, 2005.

[8] Xiao-Liang Qi, Rundong Li, Jiadong Zang, and Shou-Cheng Zhang. Inducing a magnetic monopole with topological surface states. *Science*, 323(5918):1184–1187, 2009.

[9] Liang Fu, Charles L Kane, and Eugene J Mele. Topological insulators in three dimensions. *Physical Review Letters*, 98(10):106803, 2007.

[10] Chetan Nayak, Steven H Simon, Ady Stern, Michael Freedman, and Sankar Das Sarma. Non-abelian anyons and topological quantum computation. *Reviews of Modern Physics*, 80(3):1083, 2008.

[11] Sankar Das Sarma, Michael Freedman, and Chetan Nayak. Topologically protected qubits from a possible non-abelian fractional quantum Hall state. *Physical Review Letters*, 94(16):166802, 2005.

[12] AR Mellnik, JS Lee, A Richardella, JL Grab, PJ Mintun, Mark H Fischer, Abolhassan Vaezi, Aurelien Manchon, E-A Kim, N Samarth, et al. Spin-transfer torque generated by a topological insulator. *Nature*, 511(7510):449–451, 2014.

[13] Takashi Fujita, Mansoor Bin Abdul Jalil, and Seng Ghee Tan. Topological insulator cell for memory and magnetic sensor applications. *Applied Physics Express*, 4(9): 094201, 2011.

[14] Chao-Xing Liu, Xiao-Liang Qi, HaiJun Zhang, Xi Dai, Zhong Fang, and Shou-Cheng Zhang. Model Hamiltonian for topological insulators. *Physical Review B*, 82(4): 045122, 2010.

[15] B Andrei Bernevig, Taylor L Hughes, and Shou-Cheng Zhang. Quantum spin Hall effect and topological phase transition in hgte quantum wells. *Science*, 314(5806): 1757–1761, 2006.

[16] Haijun Zhang, Chao-Xing Liu, Xiao-Liang Qi, Xi Dai, Zhong Fang, and Shou-Cheng Zhang. Topological insulators in Bi2Se3, Bi2Te3 and Sb2Te3 with a single Dirac cone on the surface. *Nature physics*, 5(6):438–442, 2009.

[17] Michel Fruchart and David Carpentier. An introduction to topological insulators. *Comptes Rendus Physique*, 14 (9):779–815, 2013.

[18] Shun-Qing Shen, Wen-Yu Shan, and Hai-Zhou Lu. Topological insulator and the Dirac equation. 1(01):33–44, 2011.

[19] Jacob A Dunningham. Quantum phase transitions: Entanglement stirred up. *Nature Physics*, 5(6):381–381, 2009.

[20] Howard Barnum, Emanuel Knill, Gerardo Ortiz, Rolando Somma, and Lorenza Viola. A subsystem-independent generalization of entanglement. *Physical Review Letters*, 92(10):107902, 2004.

[21] S Sachdev. Quantum phase transitions cambridge univ. *Press, Cambridge*, 1999.

[22] SL Sondhi, SM Girvin, JP Carini, and D Shahar. Continuous quantum phase transitions. *Reviews of Modern Physics*, 69(1):315, 1997.

[23] Liang Fu. Hexagonal warping effects in the surface states of the topological insulator bi 2 te 3. *Physical review letters*, 103(26):266801, 2009.

[24] M Zahid Hasan and Charles L Kane. Colloquium: topological insulators. *Reviews of Modern Physics*, 82(4): 3045, 2010.

[25] E Sriram Prasath, Sreraman Muralidharan, Chiranjib Mitra, and Prasanta K Panigrahi. Multipartite entangled magnon states as quantum communication channels. *Quantum Information Processing*, 11(2):397–410, 2012.

[26] Harkirat Singh, Tanmoy Chakraborty, Prasanta K Panigrahi, and Chiranjib Mitra. Experimental estimation of discord in an antiferromagnetic heisenberg compound\ hbox {Cu}(\ hbox {NO} _ {3}) _ {2}\ cdot 2.5\,\ hbox {H} _ {2}\ hbox {O}. *Quantum Information Processing*, 14(3):951–961, 2015.

[27] William K Wootters. Entanglement of formation of an arbitrary state of two qubits. *Physical Review Letters*, 80 (10):2245, 1998.

[28] Diptaranjan Das, Harkirat Singh, Tanmoy Chakraborty, Radha Krishna Gopal, and Chiranjib Mitra. Experimental detection of quantum information sharing and its quantification in quantum spin systems. *New Journal of Physics*, 15(1):013047, 2013.

[29] G Tkachov and EM Hankiewicz. Spin-helical transport in normal and superconducting topological insulators. *physica status solidi (b)*, 250(2):215–232, 2013.

[30] Supriyo Datta. *Electronic transport in mesoscopic systems*. Cambridge university press, 1997.

[31] Christoph Brüne, Andreas Roth, Hartmut Buhmann,

Ewelina M Hankiewicz, Laurens W Molenkamp, Joseph Maciejko, Xiao-Liang Qi, and Shou-Cheng Zhang. Spin polarization of the quantum spin Hall edge states. *Nature Physics*, 8(6):485–490, 2012.